

This item is the archived peer-reviewed author-version of:

First mitochondrial genomes of five hoverfly species of the genus *Eristalinus* (Diptera: Syrphidae)

Reference:

Sonet Gontran, De Smet Yannick, Tang Min, Virgilio Massimiliano, Young Andrew Donovan, Skevington Jeffrey H., Mengual Ximo, Backeljau Thierry, Liu Shanlin, Zhou Xin,- First mitochondrial genomes of five hoverfly species of the genus *Eristalinus* (Diptera: Syrphidae)
Genome - ISSN 0831-2796 - 62:10(2019), p. 677-687
Full text (Publisher's DOI): <https://doi.org/10.1139/GEN-2019-0009>

1 **First mitochondrial genomes of five hoverfly species of the genus *Eristalinus***

2 **(Diptera: Syrphidae)**

3
4 Gontran Sonet^{1*}, Yannick De Smet², Min Tang³, Massimiliano Virgilio², Andrew Donovan Young^{4,5},
5 Jeffrey H. Skevington^{6,7}, Ximo Mengual⁸, Thierry Backeljau^{1,9}, Shanlin Liu¹⁰, Xin Zhou³, Marc De
6 Meyer², and Kurt Jordaens^{2,9}

7
8 ¹Royal Belgian Institute of Natural Sciences, JEMU and BopCo, Vautierstraat 29, B-1000 Brussels,
9 Belgium

10 ²Royal Museum for Central Africa, JEMU and BopCo, Leuvensesteenweg 13, B-3080 Tervuren,
11 Belgium

12 ³Department of Entomology, China Agricultural University, Beijing 100193, China

13 ⁴Plant Pest Diagnostics Center, California Department of Food and Agriculture, 3294 Meadowview
14 Road, Sacramento, CA 95832, USA

15 ⁵Department of Entomology and Nematology, University of California, Davis, Briggs Hall, Davis,
16 CA 95616-5270, USA

17 ⁶Canadian National Collection of Insects, Arachnids and Nematodes, Agriculture and Agri-Food
18 Canada, K.W. Neatby Building, 960 Carling Avenue, Ottawa, ON K1A 0C6, Canada

19 ⁷Department of Biology, Carleton University, 1125 Colonel By Drive, Ottawa, ON K1S 5B6, Canada

20 ⁸Zoologisches Forschungsmuseum Alexander Koenig, Leibniz-Institut für Biodiversität der Tiere,
21 Adenauerallee 160, D-53113 Bonn, Germany

22 ⁹University of Antwerp, Evolutionary Ecology Group, Universiteitsplein 1, B-2610 Antwerp,
23 Belgium

24 ¹⁰China National GeneBank, BGI-Shenzhen, Shenzhen, Guangdong 518083, China

25 *corresponding author: Gontran Sonet – gsonet@naturalsciences.be

26 **Abstract**

27 The hoverfly genus *Eristalinus* (Diptera, Syrphidae) contains many widespread pollinators. The
28 majority of the *Eristalinus* species occur in the Afrotropics and their molecular systematics still
29 needs to be investigated. This study presents the first complete and annotated mitochondrial
30 genomes for five *Eristalinus* species. They were obtained by high-throughput sequencing of total
31 genomic DNA. The total length of the mitogenomes varied between 15,757 and 16,245 base pairs.
32 Gene composition, positions and orientation were shared across species, and were identical to those
33 observed for other Diptera. Phylogenetic analyses (maximum likelihood and Bayesian inference)
34 based on the 13 protein coding and both rRNA genes suggested that the subgenus *Eristalinus* was
35 paraphyletic with respect to the subgenus *Eristalodes*. An analysis of the phylogenetic
36 informativeness of all protein coding and rRNA genes suggested that NADH dehydrogenase
37 subunit 5 (*nad5*), cytochrome *c* oxidase subunit 1, *nad4*, *nad2*, cytochrome *b* and 16S rRNA genes
38 are the most promising mitochondrial molecular markers to result in supported phylogenetic
39 hypotheses of the genus. In addition to the five complete mitogenomes currently available for
40 hoverflies, the five mitogenomes published here will be useful for broader molecular phylogenetic
41 analyses among hoverflies.

42
43 **Key words:** flower fly; mitogenome; phylogenetic informativeness; phylogeny

44

45 **Introduction**

46 Four subfamilies are recognized in the family Syrphidae (Insecta: Diptera), also known as hoverflies
47 or flower flies: Microdontinae, Syrphinae, Eristalinae and Pipizinae (Mengual et al. 2015; Young et
48 al. 2016). Yet, the subfamily Eristalinae appears paraphyletic in relation with the three other
49 subfamilies (Hippra and Ståhls 2005; Skevington and Yeates 2000; Ståhls et al. 2003). A widespread
50 genus within the Eristalinae is *Eristalinus* Rondani, 1845. It is naturally present in all biogeographic
51 regions except in the Neotropics, although a few records indicate that it was introduced in Chile
52 (Thompson 1999). Species of this genus are large hoverflies (4–16 mm), and most of them are
53 imperfect bee mimics with punctate (spotted) and/or fasciate (striped) eyes. They occur in a wide
54 variety of habitats including open grasslands, shrub lands, river valleys, forest margins, wetlands,
55 river banks, lake shores and even urban areas. Larvae can be found in small temporary waterbodies.
56 The genus comprises approximately 75 species worldwide, of which 54 occur in the Afrotropical
57 Region. It is divided into five subgenera: *Eristalinus* Rondani, 1845 (including *Lathyrophthalmus*
58 Mik, 1897), *Eristalodes* Mik, 1897, *Helophilina* Becker, 1923, *Merodonoides* Curran, 1931 and
59 *Oreristalis* Séguy, 1951. So far, the phylogenetic relationships among the *Eristalinus* species of the
60 Afrotropical Region remain unknown. A preliminary phylogenetic study on *Eristalinus* species from
61 the Afrotropics using three mitochondrial (cytochrome *c* oxidase subunit 1, cytochrome *b* and 12S
62 rRNA) and two nuclear (18S and 28S rRNA) gene fragments showed low support for many nodes in
63 the phylogenetic trees (De Smet et al. unpublished results) prompting the usage of additional DNA
64 markers to resolve species and subgenus relationships within *Eristalinus*. Phylogenetic studies using
65 whole mitochondrial genomes (mitogenomes) have shown the potential to tackle phylogenetic issues
66 at varying taxonomic levels (*e.g.* Cameron 2013; Cameron et al. 2007, 2009; Ma et al. 2012; Nelson
67 et al. 2012; Yong et al. 2015). The objectives of the current study are to assemble the mitogenomes
68 of five Afrotropical *Eristalinus* species (belonging to two subgenera), infer their phylogenetic
69 relationships and measure the informativeness of each mitochondrial protein coding gene (PCG) and
70 rRNA gene for the resolution of phylogenetic relationships within *Eristalinus*.

71

72 **Materials and methods**

73 Total genomic DNA was extracted from five Afrotropical *Eristalinus* specimens of the subgenera
74 *Eristalinus* and *Eristalodes*, viz. *Eristalinus* (*Eristalinus*) *aeneus* (Scopoli, 1763), *Eristalinus*
75 (*Eristalinus*) *tabanoides* (Jaenicke, 1867), *Eristalinus* (*Eristalinus*) *vicarians* (Bezzi, 1915),
76 *Eristalinus* (*Eristalodes*) *barclayi* (Bezzi, 1915) and *Eristalinus* (*Eristalodes*) *fuscicornis* (Karsch,
77 1887) (Table 1), using the DNeasy® Blood & Tissue kit (Qiagen Inc., Hilden, Germany). Specimens
78 were collected between October 2012 and May 2014 and stored in absolute ethanol. To minimize
79 contamination with exogenous DNA, three legs were extracted from each specimen, rinsed in
80 absolute ethanol and air dried for 10 minutes at 50 °C before DNA extraction. DNA concentrations
81 of the extracts were measured with Qubit 2.0 (ThermoFisher Scientific, Waltham, Massachusetts,
82 USA) and ranged between 13 and 60 ng/μl.

83 One DNA library was prepared following the Illumina® TruSeq® DNA Sample Preparation
84 Kit. An insert size of 250 base pairs (bp) was targeted after pooling 100 ng of the genomic DNA of
85 each specimen. The DNA library was sequenced (150 bp paired-end reads) on an Illumina (San
86 Diego, California, USA) HiSeq4000 platform at BGI-Shenzhen (China). The raw data was cleaned
87 using a custom Perl script (Zhou et al. 2013) to remove Illumina adapters, reads with > 10% of low
88 quality bases (Phred-scores < 20) or with more than five unresolved bases. The remaining reads were
89 processed in the mitogenome assembly pipeline described by Tang et al. (2015). To achieve the final
90 mitogenome assembly, the source code of the assembler SOAPdenovo-Trans(-K 71, -t 1) (Xie et al.
91 2014) was modified to remove scaffold connections with read supports ≤ 10 . Mitogenomes were
92 circularized and visualized in Geneious 10.2.2 (Biomatters, Auckland, New Zealand). A first draft
93 annotation of the mitogenomes was obtained in MITOS (Bernt et al. 2013) with default settings. Then,
94 open reading frames (ORF) of the mitochondrial coding genes were inferred using the transfer RNA
95 (tRNA) punctuation principle as proposed by Cameron (2014). For this, annotations obtained from
96 MITOS were manually edited in Geneious 10.2.2. Largest ORFs found between tRNAs were selected,

97 allowing truncated (incomplete) stop codons (which are completed by RNA polyadenylation) and
98 overlap between adjacent ORFs. Limits of the currently adopted routines for mitogenomic
99 assemblage and annotation are presented by Velozo Timbó et al. (2017). The cloverleaf structure of
100 the 22 inferred tRNAs were visualized in MITOS. The assembled and annotated mitogenomes were
101 submitted to GenBank (accession numbers from MH321204 to MH321208). Gene symbols and their
102 concordance with the nomenclature of FlyBase (Gramates et al. 2017) are given in Table 2. All
103 mitogenomes were aligned in MUSCLE (Edgar, 2004).

104 Using Geneious 10.2.2, uncorrected pairwise p-distances (proportion of nucleotide sites at
105 which two sequences are different) were calculated among the mitogenomes of the five *Eristalinus*
106 specimens sequenced here and the five mitochondrial genomes of Syrphidae available in GenBank:
107 *Episyrphus balteatus* (de Geer, 1776) (GenBank accession number: NC_036481), *Eristalis tenax*
108 (Linnaeus, 1758) (MH159199), *Eupeodes corollae* (Fabricius, 1794) (NC_036482), *Ocyptamus*
109 *sativus* (Curran, 1941) (KT272862) and *Simosyrphus grandicornis* (Macquart, 1842) (NC_008754).
110 Graphs representing GC content and the similarity among the mitogenomes sequenced here were
111 made in Geneious 10.2.2 using sliding windows of 99 bp and 50 bp, respectively.

112 Phylogenetic analyses were performed using both maximum likelihood (ML) and Bayesian
113 inference (BI). For this, all PCGs and rRNA genes of the five mitogenomes obtained here and the
114 five mitogenomes of Syrphidae available in GenBank (see above) were concatenated and aligned
115 using the default parameters of ClustalW (Thompson et al. 1994). The dataset was then partitioned in
116 41 character sets corresponding to the different codon positions of the 13 PCGs (39) and the two
117 rRNA genes. Additional ML and BI analyses were performed on the basis of *cox1* and including
118 additional *Eristalinus* samples sequenced by Pérez-Banon et al. (2003). This latter dataset was
119 partitioned according to codon position. For each partition of all analyses, the General Time
120 Reversible (GTR) model was applied, and a gamma distribution was used to approximate the
121 heterogeneity of substitution rates among different sites. In all analyses (ML and BI), members of the
122 sub-family Eristalinae represented the ingroup and members of the sub-family Syrphinae were used

123 as outgroup to root the tree. ML analyses and BI were performed on the CIPRES Science Gateway
124 (Miller et al. 2010) using RAxML v. 8 (Stamatakis 2014) and MrBayes 3.2.6 (Ronquist &
125 Huelsenbeck 2003), respectively. ML analyses were implemented with autoMRE bootstrapping
126 (setting a maximum of 1000 bootstraps) (Stamatakis 2014). The Bayesian analyses consisted in two
127 runs, each with a cold chain and three incrementally heated chains. Starting trees for each chain were
128 random and the default values of MrBayes were chosen for all settings (including prior distributions).
129 MrBayes metropolis coupled Markov Chains Monte Carlo (MCMC) were run for 20 million
130 generations with heating temperature of 0.1. Trees were sampled every 1000 generations with 50%
131 of trees discarded as burn-in. Run convergence was verified by considering the average standard
132 deviation of split frequencies (Ronquist & Huelsenbeck 2003). Only nodes with posterior
133 probabilities > 0.95 (BI) and bootstrap support $> 70\%$ (ML) were considered.

134 Phylogenetic Informativeness (PI) is a quantitative measure of the ability of characters to
135 resolve phylogenetic relationships among taxa over a specified historical time scale (Townsend
136 2007). In order to identify the best mitochondrial markers for the resolution of phylogenetic
137 hypotheses within the genus *Eristalinus*, we estimated the net PI of each PCG and rRNA gene. In
138 contrast with the PI per site, the net PI summarizes the PI for a set of characters and quantifies signal
139 as a whole. The PI of single genes can be evaluated using, as prior information, more complete or
140 comparative genomic data from within or outside the taxonomic group of interest (López-Giráldez
141 and Townsend 2011). Here, we considered the concatenation of all PCGs and rRNA genes as prior
142 information. The analysis was performed by applying the HyPhy algorithm
143 (<http://phydesign.townsend.yale.edu>) (López-Giráldez and Townsend 2011) to the PCGs and rRNA
144 genes of the five *Eristalinus* species and the five mitochondrial genomes of Syrphidae available in
145 GenBank (see above). The reference ultrametric tree required by the algorithm as prior information
146 was reconstructed as a strict molecular clock tree using MrBayes v. 3.2.6 (Ronquist & Huelsenbeck
147 2003) available on the CIPRES Science Gateway (Miller et al. 2010). . Convergence was checked as
148 explained above.

149

150 **Results**

151 An average of 11.2 million reads were obtained per sample ($SD = 0.8 \times 10^6$) with high proportions of
152 reads with a Phred score ≥ 20 ($96.6 \pm 0.3\%$ for read 1; $90.6 \pm 1.0\%$ for read 2). The aligned
153 mitogenomes (File S1) ranged from 15,757 bp (*E. barclayi*) to 16,245 bp (*E. aeneus*), with most of
154 the interspecific length variation situated in the AT-rich control region (Tables 2 and 3), which, in all
155 species, was between the trnS and trnI genes (conversions of gene name abbreviations in Table 2).
156 Base composition of mitogenomes was heavily skewed towards A+T, with a GC content of 20–20.2%
157 (Table 3). Every mitogenome contained the same 37 genes, ordered identically and comprising 13
158 PCGs, two rRNA and 22 tRNA genes. The number of intergenic regions, and their cumulative length,
159 was variable among species (Table 2).

160 Nine of the 13 PCGs were situated on the H-strand (represented clockwise in Fig. 1) and four
161 on the L-strand (represented counter clockwise in Fig. 1). Lengths of coding regions and start/stop
162 codons are given in Table 2. Each PCG had the same start and stop codons in the five species with
163 the following exceptions: ATT instead of ATC as start codon for nad6 in *E. aeneus* and TAA stop
164 codon in *E. aeneus*, *E. barclayi* and *E. fuscicornis* instead of TAG in *E. tabanoides* and *E. vicarians*
165 for nad1. The most common start codon was ATG (observed in 46% of the PCG/species
166 combinations), followed by ATT (20%) and ATC (10%). Other start codons, TCG, TTG, and GTG
167 represented 8% each. The most common stop codon was TAA (54% of the PCG/species
168 combinations), while TAG was observed in 6% of the cases. An incomplete stop codon T(AA) was
169 observed in three PCGs (nad2, cox1 and nad5) of all five species, with an additional T(AA) stop
170 codon in nad3 of *E. aeneus*, *E. tabanoides* and *E. vicarians*. Another incomplete stop codon TA(A)
171 was observed in two PCGs (nad4 and nad6) of four species (all except *E. aeneus*). These incomplete
172 stop codons represented thus 28% [T(AA)] and 12% [TA(A)] of PCG/species combinations (Table
173 2).

174 Fourteen of the 22 tRNA genes were situated on the H-strand and eight on the L-strand (Table

175 2, Fig. 1). The cloverleaf structure of trnS1 lacked the D-loop in all species, while trnK and trnR
176 lacked the TΨC-loop in *E. aeneus* and *E. tabanoides*, respectively (File S2). The two rRNA genes
177 were situated on the H-strand (Table 2, Fig. 1).

178 Overlapping genes were found two times on the same strand (atp8/atp6 and nad4/nad4l), and
179 two times on different strands (trnW/trnC and trnY/cox1) in all five species. Additional overlaps were
180 observed on the same strand for nad6/cob in all species except for *E. aeneus*, and on different strands
181 for trnI/trnQ in *E. barclayi*, *E. fuscicornis* and *E. vicarians* (Table 2).

182 Uncorrected p-distances measured among the five *Eristalinus* mitogenomes (File S3) ranged
183 from 0.006 (*E. fuscicornis* – *E. barclayi*) to 0.112 (*E. aeneus* – *E. tabanoides*). Surprisingly,
184 intergeneric distances measured between *Episyrphus* and *Simosyrphus* (0.019) were relatively small
185 compared to the interspecific divergences measured within *Eristalinus*. They were also much smaller
186 than the other intergeneric distances measured within Syrphidae (ranging from 0.111 between
187 *Eristalix tenax* and *E. fuscicornis* to 0.198 between *Ocyrtamus sativus* and *Eristalinus aeneus*).

188 The phylogenetic trees reconstructed using ML and BI had almost the same topology, the only
189 difference between the two analyses being the sister relationship between *E. tabanoides* and *E.*
190 *vicarians* that is suggested by the BI but remained unresolved in the ML analysis (Fig. 2). These
191 analyses suggested that *Eristalinus aeneus* was the sister-species of the other four *Eristalinus* species
192 sampled here. It also suggested that the two species belonging to the *Eristalodes* subgenus, *E. barclayi*
193 and *E. fuscicornis*, were sister-species and formed a clade that was nested within the genus
194 *Eristalinus*, making the subgenus *Eristalinus* paraphyletic with respect to the subgenus *Eristalodes*.
195 The phylogenetic analyses (ML and BI) based on cox1 (alignment in File S4) and including the
196 additional *Eristalinus* samples sequenced by Pérez-Banon et al. (2003) were not sufficiently resolved
197 to evaluate the reciprocal monophyly of the two subgenera (Fig. 3). In these trees, *E. tabanoides* and
198 *E. megacephalus* were sister-species, and *E. vicarians* and *E. dubiosus* were sister-species. In
199 contrast, the two *E. aeneus* specimens (one of this study, one of Pérez-Banon et al. (2003)) did not
200 cluster with one another.

201 A plot of the net PI profiles on the same time scale (x-axis) as the Bayesian phylogenetic
202 ultrametric tree obtained for the dataset including all PCGs and rRNA genes is given in Fig. 4. The
203 genes showing the highest PI profiles are *nad5*, *cox1* and *nad4*, followed by *nad2*, *cob* and 16S rRNA,
204 indicating an overall higher utility of these genes for phylogenetic inference compared to the other
205 genes such as *atp8*, *nad4l*, *nad3* and 12S rRNA, which had flatter PI profiles (Fig. 4). For most genes,
206 the optima of the PI profiles were situated after the divergence between *E. aeneus* and the other
207 *Eristalinus* representatives. This means that, for these genes, character changes (mutations) were
208 estimated to mainly occur along the branches of the subtree corresponding to the *Eristalinus* genus.
209 These genes are therefore more promising to resolve intrageneric relationships. For several genes,
210 especially for 16S rRNA, the PI profile also showed a narrow peak next to the tips of the tree (between
211 the bipartition leading to *Episyrphus balteatus* and *Simosyrphus grandicornis* and the bipartition
212 leading to *Eristalinus barclayi* and *E. fuscicornis*). These genes may therefore have a relatively higher
213 power to resolve more recent divergences.

214

215 Discussion

216 This study presents the first complete and annotated mitogenomes for the hoverfly genus *Eristalinus*.
217 The only other published mitogenomes of Syrphidae are from one species of the sub-family
218 Eristalinae, *Eristalis tenax* (Li et al. 2017), and four species of the sub-family Syrphinae: *Episyrphus*
219 *balteatus* and *Eupeodes corollae* (Pu et al. 2017), *Ocyptamus sativus* and *Simosyrphus grandicornis*
220 (Junqueira et al. 2016), and the partial mitogenome of an unknown species “Syrphidae sp.” (Tang et
221 al. 2014, accession number: KM244713). Mitogenome sizes of *Eristalinus* (15,757 – 16,245 bp) are
222 comparable to those already published for the family (15,214 – 16,175 bp, see Table 3), with *E.*
223 *aeneus* showing the largest published Syrphidae genome to date (16,245 bp). Gene order is identical
224 in all Syrphidae and in line with previously reported dipteran mitogenomes (e.g., Li et al. 2017; Pu et
225 al. 2017; Yong et al. 2015). This result is not surprising because gene composition and order is well
226 conserved within Diptera (Wolstenholme 1992) even if cases of tRNA gene duplication have been

227 observed within the family Calliphoridae (Duarte et al. 2008; Junqueira et al. 2004).

228 The mitogenomes obtained in this study show a promising array of diversity across the genus
229 *Eristalinus*, with both large p-distances (between *E. aeneus* and the other *Eristalinus* species) and
230 remarkably low pairwise p-distance between the two representatives of the subgenus *Eristalodes* (File
231 S3), suggesting a close relationship between both species. The latter is corroborated with species
232 delimitation methods applied to mitochondrial and nuclear markers which show that *E. barclayi* and
233 *E. fuscicornis* form a species-complex, also comprising *Eristalinus quinquelineatus* (Fabricius, 1797)
234 (De Smet et al. unpublished data). These results either question the taxonomic value of the
235 morphological characters used to distinguish the three species, or illustrates a recent divergence,
236 ongoing speciation, hybridization or introgression. The phylogenetic analyses of the mitogenomes of
237 the five *Eristalinus* species suggest that the subgenera *Eristalinus* and *Eristalodes* are not reciprocally
238 monophyletic. Indeed, the subgenus *Eristalodes* renders the subgenus *Eristalinus* paraphyletic (Fig.
239 2). In a phylogenetic study (parsimony analysis) of five *Eristalinus* species based on *cox1* and the
240 28S rRNA gene (Pérez-Bañón et al. 2003), *E. taeniops*, the species type of the subgenus *Eristalodes*
241 was nested within the subgenus *Eristalinus*. The lack of resolution of the phylogenetic trees obtained
242 here using *cox1* only (Fig. 3), does not contribute to solve this question. However, since our study
243 and that of Pérez-Bañón et al. (2003) only included a limited number of species of the subgenus
244 *Eristalodes*, more comprehensive phylogenetic analyses, including more species of both subgenera
245 and species of the remaining three subgenera, are needed to test for the subgeneric rank of the different
246 subgenera in this genus. The phylogenetic trees based on *cox1* (Fig. 3) also revealed that the
247 specimens identified as *E. aeneus* here in and in the study of Pérez-Bañón et al. (2003) may belong
248 to different lineages. This species has a very wide distribution and probably may comprise cryptic
249 species.

250 Assessing the PI profiles for all PCGs within the genus *Eristalinus* revealed substantial
251 difference in their suggested utility for phylogeny reconstruction (Fig. 4. Some mitochondrial markers
252 (*nad5*, *cox1*, *nad4*, *nad2*, *cob* and the 16S rRNA gene) exhibit higher PI profiles, especially for the

253 time range corresponding to the diversification of the *Eristalinus* species considered here. The utility
254 of mitogenomics for the study of insect evolution and phylogeny has been amply demonstrated
255 (Cameron, 2013). Mitogenomes are available for all insect orders and have been shown to hold
256 phylogenetic information over extensive taxonomic scales (*e.g.*, Cameron et al. 2007, 2009; Logue et
257 al. 2013; Ma et al. 2012; Nelson et al. 2012; Zhao et al. 2013). These results suggest that the
258 sequencing of the mitogenomes of additional syrphid species would be useful to investigate the
259 systematics of the family and clarify the classification within *Eristalinus*.

260

261 **Acknowledgements**

262 GS, YDS, MV, TB, MDM and KJ acknowledge financial support of the Belgian Science Policy
263 (BELSPO) for part of this work through the Joint Experimental Molecular Unit (JEMU), the
264 Barcoding Facility for Organisms and Tissues of Policy Concern (BopCo), and the project
265 BR/314//PI/SYRPINTINE to KJ. Research work was done with IITA and is based on bilateral
266 agreements in form of memorandums of understanding (MoU) signed by the ministries of agriculture
267 of the respective countries (more information can be found on <http://www.iita.org/>). In this
268 framework, research work in the field is an integral part of IITA's contracted mandate. Therefore, no
269 specific permissions were required for the collected hoverfly material. None of the hoverfly species
270 figure in any red list, are endangered, threatened or considered to be endangered in the involved
271 countries. No species collected in the present study are ranked in any IUCN list or are protected by
272 CITES. The authors thank the reviewers for their pertinent suggestions.

273

274 **References**

275 Bernt, M., Donath, A., Jühling, F., Externbrink, F., Florentz, C., Fritzsche, G., Pütz, J., Middendorf,
276 M., and Stadler, P.F. 2013. MITOS: improved *de novo* metazoan mitochondrial genome
277 annotation. *Mol. Phylogenet. Evol.* **69**(2): 313–319. doi:10.1016/j.ympev.2012.08.023.
278 PMID:22982435.

- 279 Cameron, S.L. 2013. Insect mitochondrial genomics: Implications for evolution and phylogeny.
280 *Annu. Rev. Entomol.* **59**(1): 95–117. doi:10.1146/annurev-ento-011613-162007.
- 281 Cameron, S.L. 2014. How to sequence and annotate insect mitochondrial genomes for systematic and
282 comparative genomics research. *Syst. Entomol.* **39**(3): 400–411. doi:10.1111/syen.12071.
- 283 Cameron, S.L., Lambkin, C.L., Barker, S.C., and Whiting, M.F. 2007. A mitochondrial genome
284 phylogeny of Diptera: Whole genome sequence data accurately resolve relationships over broad
285 timescales with high precision. *Syst. Entomol.* **32**(1): 40–59. doi:10.1111/j.1365-
286 3113.2006.00355.x.
- 287 Cameron, S.L., Sullivan, J., Song, H., Miller, K.B., and Whiting, M.F. 2009. A mitochondrial genome
288 phylogeny of the Neuropterida (lace-wings, alderflies and snakeflies) and their relationship to
289 the other holometabolous insect orders. *Zool. Scr.* **38**(6): 575–590. doi:10.1111/j.1463-
290 6409.2009.00392.x.
- 291 Duarte, G.T., De Azeredo-Espin, A.M. and Junqueira, A.C. 2008. The mitochondrial control region
292 of blowflies (Diptera: Calliphoridae): a hot spot for mitochondrial genome rearrangements. *J.*
293 *Med. Entomol.* **45**(4):667–76. doi: 10.1603/0022-2585(2008)45[667:TMCROB]2.0.CO;2.
- 294 Edgar, R.C. 2004. MUSCLE: multiple sequence alignment with high accuracy and high throughput.
295 *Nucleic Acids Res.* **32**(5): 1792–1797. doi:10.1093/nar/gkh340. PMID:15034147.
- 296 Gramates, L.S., Marygold, S.J., dos Santos, G., Urbano, J.-M., Antonazzo, G., Matthews, B.B., Rey,
297 A.J., Tabone, C.J., Crosby, M.A., Emmert, D.B., Falls, K., Goodman, J.L., Hu, Y., Ponting, L.,
298 Schroeder, A.J., Strelets, V.B., Thurmond, J., Zhou, P., and the FlyBase Consortium. 2017.
299 FlyBase at 25: looking to the future. *Nucleic Acids Res.* **45**(Database issue): D663–D671.
300 doi:10.1093/nar/gkw1016. PMID:27799470.
- 301 Hippa, H., and Ståhls, G. 2005. Morphological characters of adult Syrphidae: Descriptions and
302 phylogenetic utility. *Acta Zool. Fenn.* **215**: 1–72. Junqueira, A.C., Azeredo-Espin, A.M., Paulo,
303 D.F., Marinho, M.A., Tomsho, L.P., Drautz-Moses, D.I., Purbojati, R.W., Ratan, A., and
304 Schuster, S.C. 2016. Large-scale mitogenomics enables insights into Schizophora (Diptera)

- 305 radiation and population diversity. *Sci. Rep.* **6**: 21762. doi:10.1038/srep21762.
306 PMID:26912394.
- 307 Junqueira, A.C., Lessinger, A.C., Torres, T.T., da Silva, F.R., Vettore, A.L., Arruda, P., and Azeredo
308 Espin, A.M. 2004. The mitochondrial genome of the blowfly *Chrysomya chloropyga* (Diptera:
309 Calliphoridae). *Gene* **15**(339): 7–15. doi: 10.1016/j.gene.2004.06.031.Li, X., Ding, S., Li, X.,
310 Peng, H., Tang, C., and Yang, D. 2017. The complete mitochondrial genome analysis of
311 *Eristalis tenax* (Diptera, Syrphidae). *Mitochondrial DNA, part B* **2**(2): 654–655.
312 doi:10.1080/23802359.2017.1375875.
- 313 Logue, K., Chan, E.R., Phipps, R., Small, S., Reimer, L., Henry-Halldi, C., Sattabongkot, J., Siba,
314 P.M., Zimmerman, P.A., and Serre, D. 2013. Mitochondrial genome sequences reveal deep
315 divergences among *Anopheles punctulatus* sibling species in Papua New Guinea. *Malar. J.* **12**:
316 64. doi:10.1186/1475-2875-12-64. PMID:23405960.
- 317 López-Giráldez F., and Townsend J.P. 2011. PhyDesign: an online application for profiling
318 phylogenetic informativeness. *BMC Evol. Biol.* **11**: 152. doi:10.1186/1471-2148-11-152.
319 PMID:21627831.
- 320 Ma, C., Yang, P.C., Jiang, F., Chapuis, M.-P., Shall, Y., Sword, G.A., and Kang, L. 2012.
321 Mitochondrial genomes reveal the global phylogeography and dispersal routes of the migratory
322 locust. *Mol. Ecol.* **21**(17): 4344–4358. doi:10.1111/j.1365-294X.2012.05684.x.
323 PMID:22738353.
- 324 Mengual, X., Ståhls, G., and Rojo, S. 2015. Phylogenetic relationships and taxonomic ranking of
325 pipizine flower flies (Diptera: Syrphidae) with implications for the evolution of aphidophagy.
326 *Cladistics*, **31**(5): 491–508. doi:10.1111/cla.12105.
- 327 Miller, M.A., Pfeiffer, W., and Schwartz, T. 2010. Creating the CIPRES Science Gateway for
328 inference of large phylogenetic trees. *In* Proceedings of the Gateway Computing Environments
329 Workshop (GCE), New Orleans, Louisiana, 14 November 2010. Institute of Electrical and
330 Electronics Engineers (IEEE), New Orleans, Louisiana. pp. 1–8.

- 331 Nelson, L.A., Lambkin, C.L., Batterham, P., Wallman, J.F., Dowton, M., Whiting, M.F., Yeates,
332 D.K., and Cameron, S.L. 2012. Beyond barcoding: genomic approaches to molecular
333 diagnostics in blowflies (Diptera: Calliphoridae). *Gene*, **511**(2): 131–142.
334 doi:10.1016/j.gene.2012.09.103.
- 335 Pérez-Bañón, C., Rojo, S., Ståhls, G., and Marcos-García, M.A. 2003. Taxonomy of European
336 *Eristalinus* (Diptera: Syrphidae) based on larval morphology and molecular data. *Eur. J.*
337 *Entomol.* **100**(3): 417–428. doi:10.14411/eje.2003.064.
- 338 Pu, D.-q., Liu, H.-l., Gong, Y.-y., Ji, P.-c., Li, Y.-j., Mou, F.-S., and Wei, S.-j. 2017. Mitochondrial
339 genomes of the hoverflies *Episyrphus balteatus* and *Eupeodes corollae* (Diptera: Syrphidae),
340 with a phylogenetic analysis of Muscomorpha. *Sci. Rep.* **7**: 44300. doi:10.1038/srep4430.
341 PMID:28276531.
- 342 Ronquist, F., and Huelsenbeck, J.P. 2003. MrBayes 3: Bayesian phylogenetic inference under mixed
343 models. *Bioinformatics* **19**(12): 1572–1574. doi:10.1093/bioinformatics/btg180.Skevington,
344 J.H., and Yeates, D.K. 2000. Phylogeny of the Syrphoidea (Diptera) inferred from mtDNA
345 sequences and morphology with particular reference to classification of the Pipunculidae
346 (Diptera). *Mol. Phylogenet. Evol.* **16**(2): 212–224. doi:10.1006/mpev.2000.0787.
347 PMID:10942608.
- 348 Ståhls, G., Hippa, H., Rotheray, G.E., Muona, J., and Gilbert, F. 2003. Phylogeny of Syrphidae
349 (Diptera) inferred from combined analysis of molecular and morphological characters. *Syst.*
350 *Entomol.* **28**(4): 433–450. doi:10.1046/j.1365-3113.2003.00225.x.
- 351 Stamatakis, A. 2014. RAxML version 8: a tool for phylogenetic analysis and post-analysis of large
352 phylogenies. *Bioinformatics*, **30**(9): 1312–1313. doi:10.1093/bioinformatics/btu033.
- 353 Tang, M., Hardman, C.J., Ji, Y., Meng, G., Liu, S., Tan, M., Yang, S., Moss, E.D., Wang, J., Yang,
354 C., Bruce, C., Nevard, T., Potts, S.G., Zhou, X., and Yu, D.W. 2015. High-throughput
355 monitoring of wild bee diversity and abundance via mitogenomics. *Methods Ecol. Evol.* **6**(9):
356 1034–1043. doi:10.1111/2041-210X.12416. PMID:27867467.

- 357 Tang, M., Tan, M., Meng, G., Yang, S., Su, X., Liu, S., Song, W., Li, Y., Wu, Q., Zhang, A., and
358 Zhou, X. 2014. Multiplex sequencing of pooled mitochondrial genomes – a crucial step toward
359 biodiversity analysis using mito-genomics. *Nucleic Acids Res.* **42**(22): e166.
360 doi:10.1093/nar/gku917. PMID:25294837.
- 361 Tavaré, S. 1986. Some Probabilistic and Statistical Problems in the Analysis of DNA Sequences. *In*
362 *Some Mathematical Questions in Biology: DNA Sequence Analysis. Edited by R.M. Miura.*
363 *American Mathematical Society, Providence, RI, USA. pp. 57–86.*
- 364 Thompson, F.C. 1999. A key to the genera of the flower flies of the Neotropical Region including the
365 descriptions of genera and species and a glossary of taxonomic terms. *Contributions, Ent.*
366 *International.* **3**(3): 321–378.
- 367 Thompson, J.D., Higgins, D.G., and Gibson, T.J. 1994. CLUSTAL W: improving the sensitivity of
368 progressive multiple sequence alignment through sequence weighting, position-specific gap
369 penalties and weight matrix choice. *Nucleic Acids Res.* **22**(22): 4673–4680.
- 370 Townsend, J.P. 2007. Profiling phylogenetic informativeness. *Syst. Biol.* **56**(2): 222–231.
371 doi:10.1080/10635150701311362. PMID:17464879.
- 372 Velozo Timbó, R., Coiti Togawa, R., Costa, M.A., Andow, D., and Paula, D.P. 2017. Mitogenome
373 sequence accuracy using different elucidation methods. *PLoS One* **12**(6): e0179971.
374 doi:10.1371/journal.pone.0179971. PMID:28662089.
- 375 Wolstenholme, D.R. 1992. Animal mitochondrial DNA: structure and evolution. *Int. Rev. Cytol.*
376 **141**:173–216.
- 377 Xie, Y., Wu, G., Tang, J., Luo, R., Patterson, J., Liu, S., Huang, W., He, G., Gu, S., Li, S., Zhou, X.,
378 Lam, T.W., Li, Y., Xu, X., Wong, G.K., and Wang, J. 2014. SOAPdenovo-Trans: *de novo*
379 transcriptome assembly with short RNA-Seq reads. *Bioinformatics* **30**(12): 1660-1666.
380 doi:10.1093/bioinformatics/btu077. PMID: 24532719.

- 381 Yang, Z. 1993. Maximum-likelihood estimation of phylogeny from DNA sequences when
382 substitution rates differ over sites. *Mol. Biol. Evol.* **10**(6): 1396-401.
383 doi:10.1093/oxfordjournals.molbev.a040082. PMID:8277861.
- 384 Yong, H.-S., Song, S.-L., Lim, P.-E., Chan, K.-G., Chow, W.-L., and Eamsobhana, P. 2015. Complete
385 mitochondrial genome of *Bactrocera arecae* (Insecta: Tephritidae) by next generation
386 sequencing and molecular phylogeny of Dacini tribe. *Sci. Rep.* **5**: 15155.
387 doi:10.1038/srep15155. PMID:26472633.
- 388 Young, A.D., Lemmon, A.R., Skevington, J.H., Mengual, X., Ståhls, G., Reemer, M., Jordaens, K.,
389 Kelso, S., Lemmon, E.M., Hauser, M., De Meyer, M., Misof, B., and Wiegmann, B.M. 2016.
390 Anchored enrichment dataset for true flies (order Diptera) reveals insights into the phylogeny
391 of flower flies (family Syrphidae). *BMC Evol. Biol.* **16**(1): 143. doi:10.1186/s12862-016-0714-
392 0. PMID:27357120.
- 393 Zhao, Z., Su, T., Chesters, D., Wang, S., Ho, S.Y.W., Zhu, C., and Chen, X. 2013. The mitochondrial
394 genome of *Elodia flavipalpis* Aldrich (Diptera: Tachinidae) and the evolutionary timescale of
395 tachinid flies. *PLoS One* **8**(4): e61814. doi: 10.1371/journal.pone.0061814. PMID:23626734.
- 396 Zhou, X., Li, Y., Liu, S., Yang, Q., Su, X., Zhou, L., Tang, M., Fu, R., Li, J., and Huang, Q. 2013.
397 Ultra-deep sequencing enables high-fidelity recovery of biodiversity for bulk arthropod
398 samples without PCR amplification. *Gigascience* **2**(1): 4. doi: 10.1186/2047-217X-2-4.
399 PMID:23587339.
- 400

401 Table 1 Voucher numbers and collection information of the five Afrotropical *Eristalinus* specimens (Diptera,
 402 Syrphidae) used in this study.

403

404 Species	voucher no.	sex	country	region	collection date
405 subgenus <i>Eristalinus</i>					
406 <i>Eristalinus aeneus</i>	RMCA ENT000033538	female	Ethiopia	Holeta	October 2012
407 <i>Eristalinus tabanoides</i>	RMCA ENT000033541	male	Benin	Calavi	April 2014
408 <i>Eristalinus vicarians</i>	RMCA ENT000033542	female	Benin	Calavi	April 2014
409 subgenus <i>Eristalodes</i>					
410 <i>Eristalinus barclayi</i>	RMCA ENT000033539	male	Benin	Calavi	April 2014
411 <i>Eristalinus fuscicornis</i>	RMCA ENT000033540	female	Benin	Cotonou	November 2013

417

418

419 Table 2 (parts a and b): Mitogenome annotations for the five Afrotropical *Eristalinus* specimens sequenced here.

Part a		<i>Eristalinus aeneus</i>						<i>Eristalinus barclayi</i>						<i>Eristalinus fuscicornis</i>					
Gene	FlyBase Symbol*	start position	end position	size (bp)	strand†	Intergenic‡	start/stop codon	start position	end position	size (bp)	strand†	intergenic‡	start/stop codon	start position	end position	size (bp)	strand†	intergenic‡	start/stop codon
trnI(gat)	tRNA:Ile-GAT	1	66	66	H			1	66	66	H			1	66	66	H		
trnQ(ttg)	tRNA:Gln-TTG	70	138	69	L	3		64	132	69	L	-3		64	132	69	L	-3	
trnM(cat)	tRNA:Met-CAT	151	219	69	H	13		153	221	69	H	20		151	219	69	H	18	
nad2	ND2	220	1,240	1,021	H	0	ATC/T(AA)	222	1,242	1,021	H	0	ATC/T(AA)	220	1,240	1,021	H	0	ATC/T(AA)
trnW(tca)	tRNA:Trp-TCA	1,241	1,308	68	H	0		1,243	1,310	68	H	0		1,241	1,308	68	H	0	
trnC(gca)	tRNA:Cys-GCA	1,301	1,369	69	L	-8		1,303	1,371	69	L	-8		1,301	1,369	69	L	-8	
trnY(gta)	tRNA:Tyr-GTA	1,399	1,465	67	L	29		1,388	1,454	67	L	16		1,386	1,452	67	L	16	
cox1	CoI	1,464	2,997	1,534	H	-2	TCG/T(AA)	1,453	2,986	1,534	H	-2	TCG/T(AA)	1,451	2,984	1,534	H	-2	TCG/T(AA)
trnL2(taa)	tRNA:Leu-TAA	2,998	3,063	66	H	0		2,987	3,052	66	H	0		2,985	3,050	66	H	0	
cox2	CoII	3,067	3,750	684	H	3	ATG/TAA	3,059	3,742	684	H	6	ATG/TAA	3,057	3,740	684	H	6	ATG/TAA
trnK(ctt)	tRNA:Lys-CTT	3,754	3,811	58	H	3		3,744	3,814	71	H	1		3,742	3,812	71	H	1	
trnD(gtc)	tRNA:Asp-GTC	3,874	3,940	67	H	>62		3,820	3,886	67	H	5		3,826	3,892	67	H	13	
atp8	ATPase8	3,941	4,102	162	H	0	ATT/TAA	3,887	4,048	162	H	0	ATT/TAA	3,893	4,054	162	H	0	ATT/TAA
atp6	ATPase6	4,096	4,773	678	H	-7	ATG/TAA	4,042	4,719	678	H	-7	ATG/TAA	4,048	4,725	678	H	-7	ATG/TAA
cox3	CoIII	4,779	5,567	789	H	5	ATG/TAA	4,724	5,512	789	H	4	ATG/TAA	4,730	5,518	789	H	4	ATG/TAA
trnG(tcc)	tRNA:Gly-TCC	5,572	5,637	66	H	4		5,516	5,582	67	H	3		5,522	5,588	67	H	3	
nad3	ND3	5,638	5,989	352	H	0	ATT/T(AA)	5,583	5,936	354	H	0	ATT/TAG	5,589	5,942	354	H	0	ATT/TAG
trnA(tgc)	tRNA:Ala-TGC	5,990	6,057	69	H	0		5,938	6,006	69	H	1		5,944	6,012	69	H	1	
trnR(tcg)	tRNA:Arg-TCG	6,058	6,121	64	H	0		6,007	6,070	64	H	0		6,013	6,076	64	H	0	
trnN(gtt)	tRNA:Asn-GTT	6,136	6,203	68	H	14		6,076	6,142	67	H	5		6,082	6,148	67	H	5	
trnS1(gct)	tRNA:Ser-GCT	6,204	6,270	67	H	0		6,143	6,209	67	H	0		6,149	6,215	67	H	0	
trnE(ttc)	tRNA:Glu-TTC	6,273	6,339	67	H	2		6,210	6,277	68	H	0		6,216	6,283	68	H	0	
trnF(gaa)	tRNA:Phe-GAA	6,368	6,435	68	L	28		6,317	6,383	67	L	39		6,324	6,390	67	L	40	
nad5	ND5	6,436	8,167	1,732	L	0	GTG/T(AA)	6,384	8,115	1,732	L	0	GTG/T(AA)	6,391	8,122	1,732	L	0	GTG/T(AA)
trnH(gtg)	tRNA:His-GTG	8,168	8,233	66	L	0		8,116	8,181	66	L	0		8,123	8,188	66	L	0	
nad4	ND4	8,236	9,576	1,341	L	2	ATG/TAA	8,182	9,521	1,340	L	0	ATG/TA(A)	8,189	9,528	1,340	L	0	ATG/TA(A)
nad4l	ND4L	9,570	9,866	297	L	-7	ATG/TAA	9,515	9,811	297	L	-7	ATG/TAA	9,522	9,818	297	L	-7	ATG/TAA
trnT(tgt)	tRNA:Thr-TGT	9,869	9,934	66	H	2		9,814	9,879	66	H	2		9,821	9,886	66	H	2	
trnP(tgg)	tRNA:Pro-TGG	9,935	10,001	67	L	0		9,880	9,946	67	L	0		9,887	9,953	67	L	0	
nad6	ND6	10,004	10,525	522	H	2	ATT/TAA	9,949	10,473	525	H	2	ATC/TA(A)	9,956	10,480	525	H	2	ATT/TA(A)
cob	Cyt-b	10,533	11,669	1,137	H	7	ATG/TAA	10,473	11,609	1,137	H	-1	ATG/TAA	10,480	11,616	1,137	H	-1	ATG/TAA
trnS2(tga)	tRNA:Ser-TGA	11,676	11,743	68	H	6		11,622	11,689	68	H	12		11,629	11,696	68	H	12	
nad1	ND1	11,765	12,706	942	L	25	TTG/TAA	11,711	12,652	942	L	21	TTG/TAA	11,718	12,659	942	L	21	TTG/TAA
trnL1(tag)	tRNA:Leu-TAG	12,708	12,772	65	L	1		12,654	12,718	65	L	1		12,661	12,725	65	L	1	
rrnL(=16S)	lrRNA	12,773	14,120	1,348	L	0		12,719	14,056	1,338	L	0		12,726	14,063	1,338	L	0	
trnV(tac)	tRNA:Val-TAC	14,121	14,192	72	L	0		14,057	14,128	72	L	0		14,064	14,135	72	L	0	
rrnS(=12S)	srRNA	14,193	14,982	790	L	0		14,129	14,918	790	L	0		14,136	14,925	790	L	0	
controlregion	ori	14,983	16,245	1,263	H	0		14,919	15,757	839	H	0		14,926	15,815	890	H	0	

* Gene abbreviations: ATP=ATP synthase membrane subunits, Co=cytochrome oxidase subunits, Cytb=cytochrome *b*, ND=NADH dehydrogenase subunits, rRNA=ribosomal RNA gene (12S and 16S), tRNA=transfer RNA gene. † Strand: H=H-strand, L=L-strand. ‡ Intergenic: intergenic region where negative values indicate an overlap between the genes.

Part b		<i>Eristalinus tabanoides</i>						<i>Eristalinus vicarians</i>					
Gene	FlyBase Symbol*	start position	end position	size (bp)	strand†	intergenic‡	start/stop codon	start position	end position	size (bp)	strand†	intergenic‡	start/stop codon
trnI(gat)	tRNA:Ile-GAT	1	66	66	H			1	66	66	H		
trnQ(ttg)	tRNA:Gln-TTG	67	135	69	L	0		64	132	69	L	-3	
trnM(cat)	tRNA:Met-CAT	174	242	69	H	38		156	224	69	H	23	
nad2	ND2	243	1,266	1,024	H	0	ATC/T(AA)	225	1,245	1,021	H	0	ATC/T(AA)
trnW(tca)	tRNA:Trp-TCA	1,267	1,334	68	H	0		1,246	1,313	68	H	0	
trnC(gca)	tRNA:Cys-GCA	1,327	1,395	69	L	-8		1,306	1,371	66	L	-8	
trnY(gta)	tRNA:Tyr-GTA	1,446	1,512	67	L	50		1,382	1,448	67	L	10	
cox1	CoI	1,511	3,044	1,534	H	-2	TCG/T(AA)	1,447	2,980	1,534	H	-2	TCG/T(AA)
trnL2(taa)	tRNA:Leu-TAA	3,045	3,110	66	H	0		2,981	3,046	66	H	0	
cox2	CoII	3,117	3,800	684	H	6	ATG/TAA	3,055	3,738	684	H	8	ATG/TAA
trnK(ctt)	tRNA:Lys-CTT	3,802	3,872	71	H	1		3,740	3,810	71	H	1	
trnD(gtc)	tRNA:Asp-GTC	3,943	4,009	67	H	70		3,881	3,947	67	H	70	
atp8	ATPase8	4,010	4,171	162	H	0	ATT/TAA	3,948	4,109	162	H	0	ATT/TAA
atp6	ATPase6	4,165	4,842	678	H	-7	ATG/TAA	4,103	4,780	678	H	-7	ATG/TAA
cox3	CoIII	4,849	5,637	789	H	6	ATG/TAA	4,784	5,572	789	H	3	ATG/TAA
trnG(tcc)	tRNA:Gly-TCC	5,641	5,707	67	H	3		5,576	5,642	67	H	3	
nad3	ND3	5,708	6,059	352	H	0	ATT/T(AA)	5,643	5,994	352	H	0	ATT/T(AA)
trnA(tgc)	tRNA:Ala-TGC	6,060	6,128	69	H	0		5,995	6,063	69	H	0	
trnR(tcg)	tRNA:Arg-TCG	6,129	6,191	63	H	0		6,064	6,127	64	H	0	
trnN(gtt)	tRNA:Asn-GTT	6,201	6,266	66	H	9		6,152	6,218	67	H	24	
trnS1(gct)	tRNA:Ser-GCT	6,267	6,333	67	H	0		6,219	6,285	67	H	0	
trnE(ttc)	tRNA:Glu-TTC	6,334	6,401	68	H	0		6,286	6,353	68	H	0	
trnF(gaa)	tRNA:Phe-GAA	6,458	6,524	67	L	56		6,382	6,448	67	L	28	
nad5	ND5	6,525	8,256	1,732	L	0	GTG/T(AA)	6,449	8,180	1,732	L	0	GTG/T(AA)
trnH(gtg)	tRNA:His-GTG	8,257	8,322	66	L	0		8,181	8,246	66	L	0	
nad4	ND4	8,323	9,662	1,340	L	0	ATG/TA(A)	8,247	9,586	1,340	L	0	ATG/TA(A)
nad4l	ND4L	9,656	9,952	297	L	-7	ATG/TAA	9,580	9,876	297	L	-7	ATG/TAA
trnT(tgt)	tRNA:Thr-TGT	9,955	10,020	66	H	2		9,879	9,944	66	H	2	
trnP(tgg)	tRNA:Pro-TGG	10,021	10,087	67	L	0		9,945	10,011	67	L	0	
nad6	ND6	10,090	10,614	525	H	2	ATC/TA(A)	10,014	10,538	525	H	0	ATT/TA(A)
cob	Cyt-b	10,614	11,750	1,137	H	-1	ATG/TAA	10,538	11,674	1,137	H	-1	ATG/TAA
trnS2(tga)	tRNA:Ser-TGA	11,761	11,828	68	H	10		11,693	11,760	68	H	18	
nad1	ND1	11,850	12,791	942	L	21	TTG/TAG	11,782	12,723	942	L	21	TTG/TAG
trnL1(tag)	tRNA:Leu-TAG	12,793	12,857	65	L	1		12,725	12,789	65	L	1	
rrnL(=16S)	rrrRNA	12,858	14,195	1,338	L	0		12,790	14,129	1,340	L	0	
trnV(tac)	tRNA:Val-TAC	14,196	14,267	72	L	0		14,130	14,201	72	L	0	
rrnS(=12S)	srRNA	14,268	15,057	790	L	0		14,202	14,990	789	L	0	
controlregion	ori	15,058	15,792	735	H	0		14,991	15,966	976	H	0	

* Gene abbreviations: ATP=ATP synthase membrane subunits, Co=cytochrome oxidase subunits, Cytb=cytochrome *b*, ND=NADH dehydrogenase subunits, rRNA=ribosomal RNA gene (12S and 16S), tRNA=transfer RNA gene. † Strand: H=H-strand, L=L-strand. ‡ Intergenic: intergenic region where negative values indicate an overlap between the genes.

426 Table 3 Genome size (base pairs), base composition (%) and GC content (%) of the syrphid
 427 mitogenomes sequenced here and retrieved from GenBank.

428		Genome	A	T	G	C	GC	Reference
429		size (base pairs)			content			
430								
431								
432	subfamily Eristalinae							
433								
434	<i>Eristalinus tabanoides</i>	15,792	41.2	38.8	8.3	11.7	20.0	this study
435	<i>Eristalinus vicarians</i>	15,966	41.1	38.9	8.2	11.8	20.0	this study
436	<i>Eristalinus aeneus</i>	16,245	47.8	32.0	7.1	13.1	20.2	this study
437	<i>Eristalinus fuscicornis</i>	15,815	41.0	38.9	8.4	11.7	20.1	this study
438	<i>Eristalinus barclayi</i>	15,757	40.9	39.0	8.4	11.8	20.2	this study
439	<i>Eristalis tenax</i>	16,091	40.0	40.1	8.7	11.2	19.9	Li et al. (2017)
440								
441	subfamily Syrphinae							
442								
443	<i>Episyrphus balteatus</i>	16,175	39.5	40.2	8.9	11.4	20.4	Pu et al. (2017)
444	<i>Eupeodes corollae</i>	15,326	40.5	39.7	8.6	11.2	19.8	Pu et al. (2017)
445	<i>Ocyptamus sativus</i>	15,214	40.2	40.2	8.5	11.1	19.6	Junqueira et al. (2016)
446	<i>Simosyrphus grandicornis</i>	16,141	40.3	40.6	8.3	10.9	19.2	Junqueira et al. (2016)
447								
448								

449 **Figure captions**

450

451 **Figure 1.** A: Schematic representation of the complete mitogenome of *Eristalinus aeneus*. Black
452 circles represent the DNA strands with numbers indicating positions in base pairs. Protein
453 coding, rRNA and tRNA genes are represented by green arrows, red arrows and pink triangles,
454 respectively. The inner blue ring depicts the GC content (with lower values towards the center
455 of the circle). B: Similarity among the mitogenomes of the five *Eristalinus* species sequenced
456 here (mean pairwise similarity over all pairs of sequences at positions covered by a sliding
457 window of 99 bp) and GC content for each species (sliding window of 50 bp).

458 **Figure 2.** Phylogenetic trees of the six Eristalinae species (five *Eristalinus* sequenced here and one
459 *Eristalix* from GenBank) based on the concatenation of all protein coding and rRNA genes.
460 Both maximum likelihood analysis (ML) and Bayesian inference (BI) were rooted using the
461 four representatives of Syrphinae (*) available in GenBank as outgroup. Bootstrap support
462 (ML) and posterior probabilities (BI) are indicated at nodes and were collapsed when < 70%
463 and < 0.95, respectively.

464 **Figure 3.** Phylogenetic trees of the Eristalinae species sequenced here and by Pérez-Banon et al.
465 (2003), and based on *cox1*. Both maximum likelihood analysis (ML) and Bayesian inference
466 (BI) were rooted using the representatives of Syrphinae (*) as outgroup. Bootstrap support (ML)
467 and posterior probabilities (BI) are indicated at nodes and were collapsed when < 70% and <
468 0.95, respectively.

469 **Figure 4.** Net phylogenetic informativeness (PI) of each mitochondrial gene plotted through time.
470 The net PI (above) is plotted in reference to the ultrametric tree (below) constructed using the
471 concatenated sequences of all protein coding and rRNA genes and where posterior probabilities
472 are given at nodes.

473

474

475

476 **Supplementary material**

477

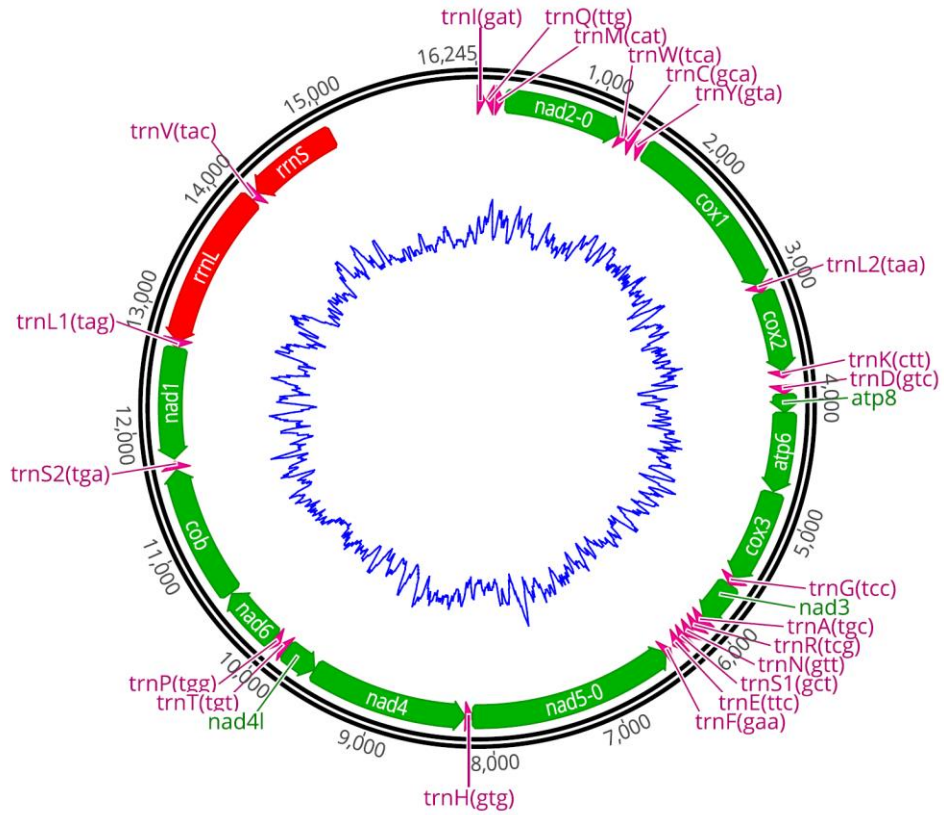
478 **File S1.** FASTA-file with the aligned complete mitogenomes of the five *Eristalinus* species and of
479 the five other syrphids included in the phylogenetic analyses [start = trnI(GAT); end = control
480 region].

481 **File S2.** Cloverleaf structure of the 22 inferred tRNAs in the mitogenome of *E. barclayi*, *E.*
482 *fuscicornis*, *E. tabanoides*, *E. vicarians* and *E. aeneus*. The cloverleaf structure for trnS1 lacked
483 the D-loop in all species, while trnK and trnR lacked the TΨC-loop in *Eristalinus aeneus* and
484 *E. tabanoides*, respectively.

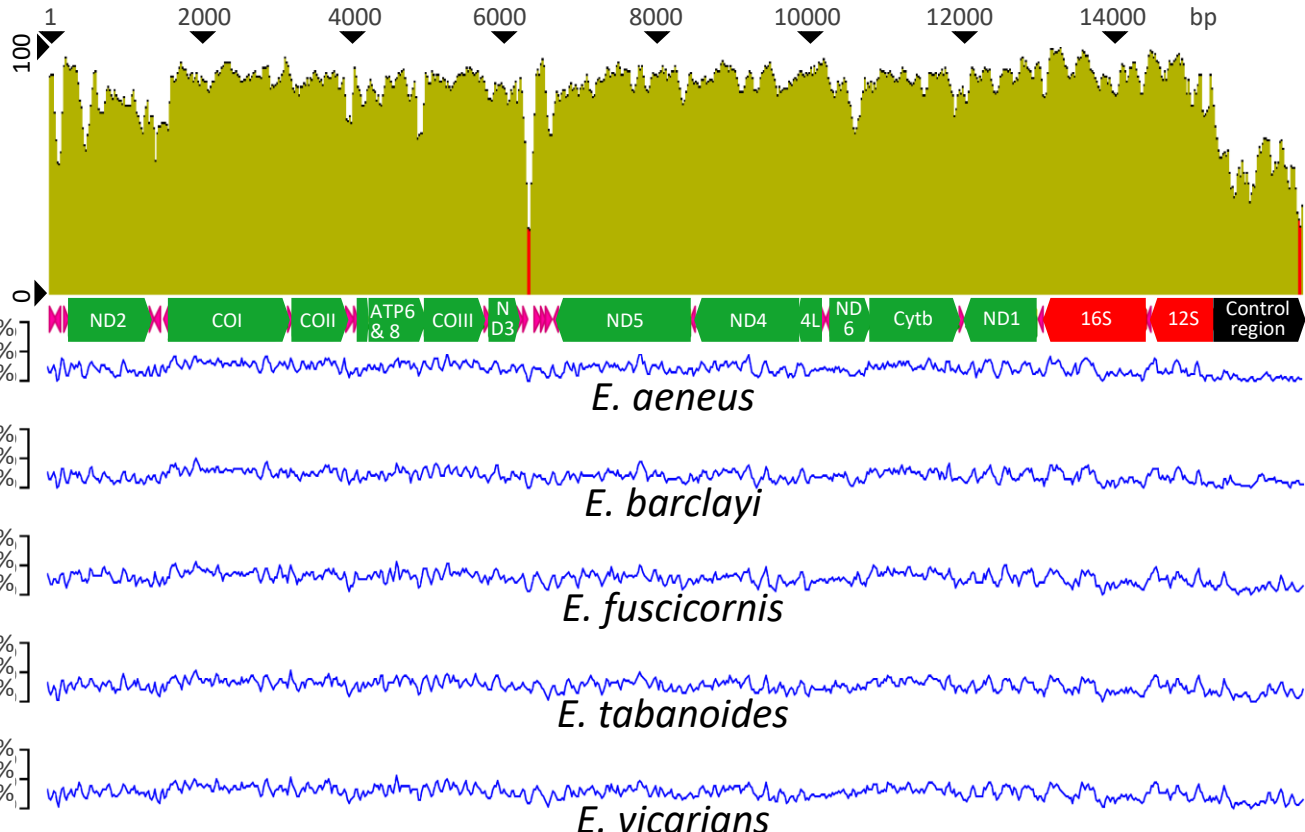
485 **File S3.** Pairwise uncorrected p-distances among the mitogenomes of the five *Eristalinus* specimens
486 sequenced here (in bold) and the five other syrphids available in GenBank.

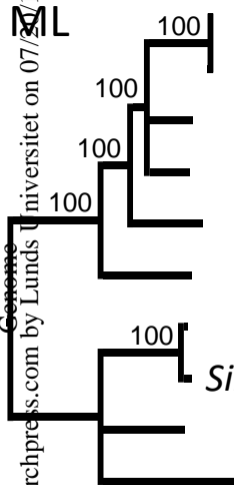
487 **File S4.** FASTA-file with the aligned cox1 sequences of the sub-family Eristalinae obtained here and
488 by Pérez-Banon et al. (2003).

A

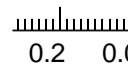
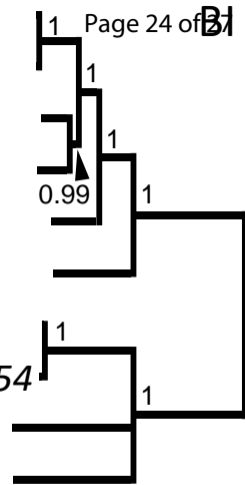
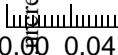


B





Eristalinus barclayi MH321205
Eristalinus fuscicornis MH321204
Eristalinus tabanooides MH321207
Eristalinus vicarians MH321206
Eristalinus aeneus MH321208
Eristalis tenax MH159199
*Episyrphus balteatus** KU351241
*Simosyrphus grandicornis** NC 008754
*Eupeodes corollae** KU379658
*Ocyrtamus sativus** KT272862



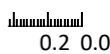
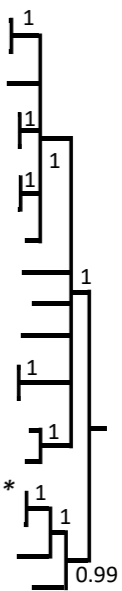
ML

Genome
www.genomerepository.com
 by Lund University on 07/20/19

Eristalinus barclayi
Eristalinus fuscicornis
Eristalinus taeniops
Eristalinus tabanoides
Eristalinus megacephalus
Eristalinus dubiosus
Eristalinus vicarians
Eristalinus aeneus
Eristalinus aeneus
Eristalinus sepulchralis
Phytomia incisa
Eristalis tenax
Eristalis tenax
Helophilus trivittatus
Myathropa florea
*Simosyrphus grandicornis**
*Episyrphus balteatus**
*Eupeodes corollae**
*Ocyptamus sativus**



BI



Genome Downloaded from www.nrcresearchpress.com by Lundsl Universitet on 07/20/19. For personal use only

Downloaded from www.nrcresearchpress.com by Lundsl Universitet on 07/20/19. For personal use only

